Contact Network Modeling of Flu Epidemics

Ian X.Y. Leung[1], Gareth Gibbs[1], Franco Bagnoli[2], Anil Sorathiya[1], and Pietro Liò[1]

[1] The Computer Laboratory, University of Cambridge, 15 JJ Thomson Avenue, Cambridge CB3 0FD, U.K.
[2] Department of Energy, University of Florence, Via S. Marta 3, 50139 Firenze, Italy; also CSDC and INFN, sez. Firenze

Abstract. Using actual census, family and age structure, land-use and population-mobility data, we develop a stochastic cellular automata on a social contact network to study the propagation of influenza epidemics in the UK. In particular, we address age dependency and obtain the contact networks through the analysis of location co-presence. We analyze infection propensities as well as vaccination techniques. The results indicate the relative merits of different vaccination strategies combined with early detection without resorting to mass vaccination of a population.

1 Introduction

The effective response to an epidemic requires an interdisciplinary and multiscale approach, exploiting aspects from individual health to population spreading patterns. Modeling epidemics has therefore been one of the most valuable tools in answering to these complex issues. Most mathematical models for the spread of disease employ differential equations based on uniform mixing assumptions or ad-hoc models for the contact process (see among others [1,2,3,4,5]).

Spatial diffusion of epidemics has been studied by means of partial differential equations or by the equivalent discretization represented by cellular automata on a regular lattice. The cellular automata method has the advantage of allowing arbitrary transitions among states, thus making easier the modeling of a plausible disease evolution, and to make possible the inclusion of quenched disorder, e.g., geographic constraints.

On the other hand, highly transmissible epidemics like flu are better modelled on the social network of contacts, which is more important than the geographic distance between any two people. However, the determination of the social network from available data is far from being trivial. Another possibility is that of resorting to agent-based modeling, following each agent during its displacements. This is expensive in computational terms, while the additional level of accuracy in the description is rarely justified by available experimental data. Eubank et al. have employed TRANSIMS [6] for modeling transport infrastructure, and built EPISIMS[7] for simulating disease spread. Other examples can be found in Refs. [8,9,10].

We employ here a cellular automata model of epidemics on an effective social network that is constructed by considering the actual interactions as the time

H. Umeo et al. (Eds): ACRI 2008, LNCS 5191, pp. 354–361, 2008.
© Springer-Verlag Berlin Heidelberg 2008

average of the persistence of individuals being in the same location. Our model utilises large-scale demographic and mobility data based on actual census and land-use. Notably, Brownstein [11] showed that influenza spread firstly in children aged 3-4 years old. Following these findings and data from HPA [12], our model considers that flu season begins with preschoolers.

2 Methodology

We consider a generalized cellular automata model in which the cells or nodes are the individuals, and the connections are defined by an adjacency matrix $J_{ij} \in \{0, 1\}$. In a regular lattice, J_{ij} is translationally invariant.

The individual variable x_i corresponds to the disease states: susceptible (S), exposed (E), infectious (I), recovered (R). Each individual has moreover a set of properties such as age, residential place, work place, etc. This can be considered equivalent to a quenched disorder.

Susceptible individuals may become exposed to the disease with probability $P_{E|S}$ if they come into "significant" contact with infected individuals through the contact networks. This transition probability also depends on some external parameters such as the virulence V of the flu strain and a seasonal factor T, that may be used to tune the simulations. Exposed individual may become infectious after an incubation period (given by the inverse of the incubation rate $P_{I|E}$); the recovery rate given by the inverse of the probability $P_{R|I}$ governs the average length of the infectious period. Vaccinated individuals are also considered recovered. The model thus belongs to the class of SEIR model [13], in which the crucial parameter is the asymptotic fraction of exposed people after the epidemic has become extinct.

One of the main points of our study is to construct the people-people social contact network J_{ij} using locations, ages, residential and work places, and considering the time that two people spend together, in average, in such places. In principle, J_{ij} should be considered a weighted matrix. Due to the lack of precise data, we set a threshold and classify contacts in two classes, "important ones" ($J_{ij} = 1$) and "influent" ones ($J_{ij} = 0$). Moreover, we distinguish the contact network according to the location k, so $J_{ij}(k) = 1$ if, in average, people i and j are expected to spend daily a significant fraction of time in location k.

2.1 Generating the Contact Network

In generating the set of people in the simulation, we utilise actual statistics as well as certain assumptions. For instance, people under 21 years old are more inclined to attend school or college rather than going to work. The age groups of the population are split into the following: 0-4, 5-14, 15-21, 22-44, 45-64, 65-90 (and above). The simulated age distribution of the population corresponds to actual statistics from the UK Census 2001[1], as depicted in Figure 1 (left). The probability of each age group is then calculated accordingly.

[1] http://www.statistics.gov.uk/

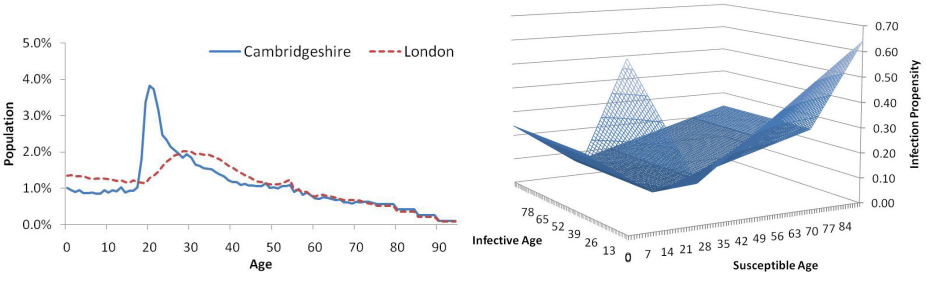

Fig. 1. Population Structure of Cambridgeshire and London (*left*). Pairwise infection propensity varies with age (*right*).

If person i goes to location k, an edge T_{ik} is drawn. We could also extend this definition by weighing the link with the time spent in the location, and considering time coincidence. However, due to the lack of precise data, we just consider the average one-day window, and set $T_{ik} = 1$ is the person is expected to spend more than one hour in that location. The effective social contact network J_{ij} is then obtained as

$$J_{ij}(k) = T_{ik}T_{jk}. \tag{1}$$

The major characteristic of our system is the division of locations into three distinct groups - public places, workplaces/schools and families. Intuitively, individuals are restricted to travel to certain locations according to their age. Four workplace/school types, one for each of the first four age groups, are explicitly represented in our model. Most individuals of age 0-64 are assumed to attend one school or to work in one workplace. Public place degree and work place degree are assumed to be normally distributed with means 3 and 1, respectively, both with variance 1. Elderly of age 65 or above is assumed retired and can only go to public places.

As suggested by EPISIMS [7], the degree distribution of locations obeys a power law distribution with an exponent, γ, of roughly 2.8. Since the number of edges is equal to the sum of all individuals' degrees (which can be calculated by the population data and the above assumptions), the degree distributions of public places and workplaces are estimated as follows:

$$n_i = c|L|i^{-\gamma}; \tag{2}$$

$$c = \left(\sum_{i=d_0}^{d_1} i^{-\gamma}\right)^{-1}, \qquad \text{since} \qquad \sum_{i=d_0}^{d_1} n_i = |L|; \tag{3}$$

$$|L| = \frac{\gamma - 2}{\gamma - 1} \cdot \frac{\sum_{p \in P} \mathrm{Deg}(p)}{d_0}, \tag{4}$$

where n_i is the number of locations with degree i, L and P are the set of locations and people, $\mathrm{Deg}(p)$ is the degree of the person $p \in P$, d_0 and d_1 are the minimum and maximum degree of any location. Effectively, each person on

average is involved in total five contact networks from the three respective types of locations. Apart from the family contact network which is generated based on household statistics, the other networks are generated according to the above estimated degree distributions. Note that d_1 can be estimated by $d_0 \cdot |L|^{\frac{1}{\beta}}$. After the set L and P are generated with their respective degrees, the probability of the existence of an edge between any $p \in P$ and $l \in L$ is $\mathrm{Deg}(p) \cdot \mathrm{Deg}(l)/\sigma$ where σ is the total number of edges.

2.2 Disease Spreading and Intervention Mechanisms

The disease starts to spread through the social contact networks within the outbreak area after parameter initialisations (initial infective, virulence, incubation rate and recovery rate), followed by diffusions to other areas. In estimating the probability of a susceptible becoming exposed, we first define the notion of pairwise propensity of infection $Q(i, s)$ between a susceptible of age s and infective of age i:

$$Q(i, s) = \mathrm{Inf}(i) \cdot \mathrm{Sus}(s) \cdot V \cdot T, \tag{5}$$

where $\mathrm{Inf}(i)$ is the typical infectivity at age i and $\mathrm{Sus}(s)$ is the typical susceptibility at age s. An example of how pairwise infection propensity varies with infectives and susceptibles of different age is depicted in Figure 1 (right). In this case they are estimated by some linear functions and can be easily further refined. Since certain viruses are known to be more persistent and pathogenic than others [14], we attempt to capture this concept by incorporating V, the virulence of the virus. Time of the year, described by the seasonal factor T, is also known to contribute largely to the prevalence of influenza[15]. For our purpose, T are V are assumed to be constant. To estimate the overall probability $P_{E|S}(s, l)$ of susceptible of age s catching the disease in the location l, we take the normalised summation of the above pairwise infection propensity:

$$P_{E|S}(s, l) = \frac{\sum_i J_{is}(l) \cdot Q(i, s)}{\mathrm{Deg}(l)}. \tag{6}$$

Noticeably, the probability of catching the disease in each neighbourhood should be proportional to the time of stay. An individual has more chance to contact with family members and colleagues than a stranger in say the same shopping center due to the spatial size of the location. Since the degree of a location somewhat reflects the spatial size and therefore the chance for a close contact with an infective, we see how the above formulation is more sensitive to the presence of infectives in a smaller place than a larger one.

The granularity of an area is crucial to the feasibility of the model. According to the UK Census 2001, Output Areas(OAs) are based on postcodes normally with size larger than 100 households. All the data used in simulation are based on the OAs area level.In modeling the disease spread across areas, we look at both the population density data and the UK national travel survey [16] which contains traffic information on an area level. We then estimate the number of individuals that are likely to travel to different areas every day. Needless to say, they may either take out or bring back the flu with them.

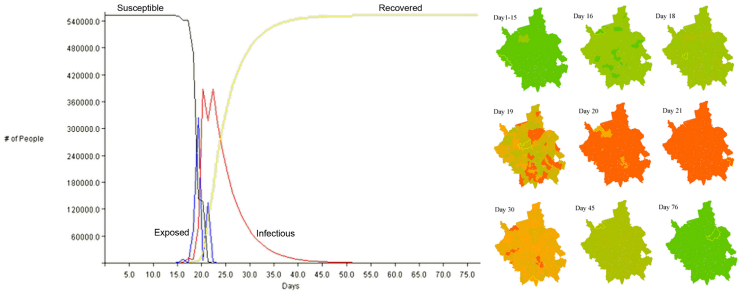

Fig. 2. A typical infective-time graph (*left*) and the corresponding epidemic spread in areas (*right*)

Three types of vaccination programs are defined in the model: age-prioritised, targeted and randomised regional vaccination. The first one prioritises on vaccinating a particular age group; the second attempts to vaccinate those who have co-located with an infective whilst the last one is completely random. It may well be argued that none of these schemes is realistic. In real world scenarios, an epidemic would often have started before it was discovered by authorities. Tracing for say those who have contacted the infectives may not be as easily done as on a computer model. Vaccine of particular type may also not be effective against the prevalent type of virus. Nonetheless, we think this will help in understanding different containment strategies and thereby preventing epidemics from developing into a worldwide pandemic.

3 Results and Discussion

We have focused on the spread of influenza in England. The main simulation is carried out in the county Cambridgeshire.

Figure 2 depicts a typical spread as modelled in our system. The peak of the exposed people curve is followed by the peak of the curve for number of infectious people. To ease the comparisons, we define the impact of an epidemic to be the sum of infected and exposed individuals per day across the whole period (the sum of the areas under the infective and exposed population curves). Two key assumptions made in the following discussions are that exposed individuals are allowed to recover directly, without being infectious; and vaccination is only effective to susceptible individuals.

With the recovery rate fixed at 0.3, we first look at the effect on the impact of varying the virulence and incubation rate as shown on the left part of Figure 3. The impact surface is plotted by 10,000 data points to smooth out the randomness. It is clear that the total impact of the epidemic increases with both the incubation rate and the virulence of the virus. Based on the assumptions, we see that the total impact increases with both incubation rate and virulence from certain critical combinations with a gradually decreasing steepness (a very different distribution is seen if less or none exposed individuals are allowed to

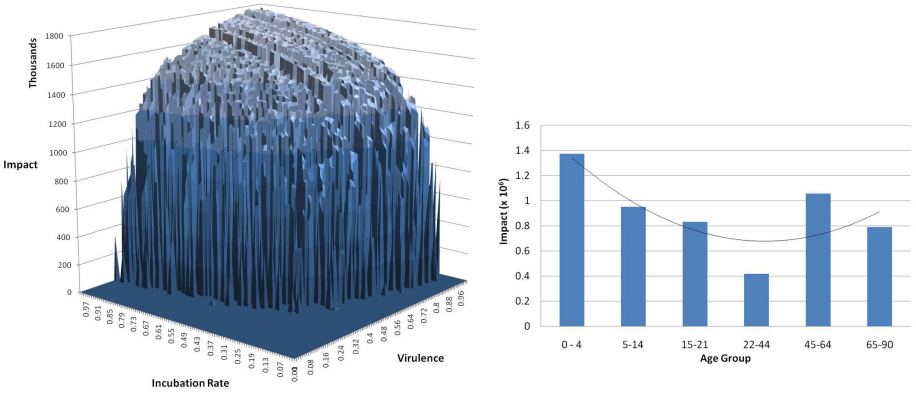

Fig. 3. Effect of virulence, incubation rate (*left*) and initial infective age (*right*) on Impact

recover directly, without being infectious). All 10000 runs are assumed to have only one random initial infective. Randomness described by the large number of dents on the surface accounts for majority cases of self-contained spreading of virus in real life scenarios, even when the virulence is high.

The right part of Figure 3 depicts the impact of an epidemic caused by initial infectives of different ages over 10 repetitions with $V = 1$, incubation rate = 0.5 and recovery rate = 0.3. The reader may wonder why the discrepancies occur when, as we have just seen, the total impact distribution should be independent of the initial infective's age. The reason is that this average is dominated by the number of "successful" epidemics over the 10 repetitions. In simpler terms, a potential epidemic is more likely to be "successful" if the initial infective is of age 0-4 given the current settings.

Lastly, we compare the three vaccination strategies. An *area*-wide threshold percentage of infections(delay threshold) is used to trigger a *region*-wide vaccination program to simulate the delay caused by imperfect monitoring. Vaccination supply is constrained by giving each area per day a number of vaccinations proportional to its population (vaccination percentage). For instance, 50% allows the area to be completely vaccinated in 2 days. We again assume that $V = 1$, incubation rate = 0.5, recovery rate = 0.3 and the vaccinations are 100% effective on individuals of all age. Suppose we know that the epidemic is started off by a 3 year old child, we plot the respective impacts for the three strategies against the vaccination percentage and the delay threshold. Predictably, as shown in the top part of Figure 4, a smaller delay threshold and faster rate of vaccination always resulted in the least impacts on all three cases. To compare the three strategies, we look at the three pairwise difference charts between them in the bottom part of the figure. A colour corresponding to the top diagrams is used to show the strategy that performed better (resulted in *less* impact) in that specific setting. In general, targeted vaccination outperformed the other two when both the delay threshold and vaccination percentage are low. The supremacy of targeted

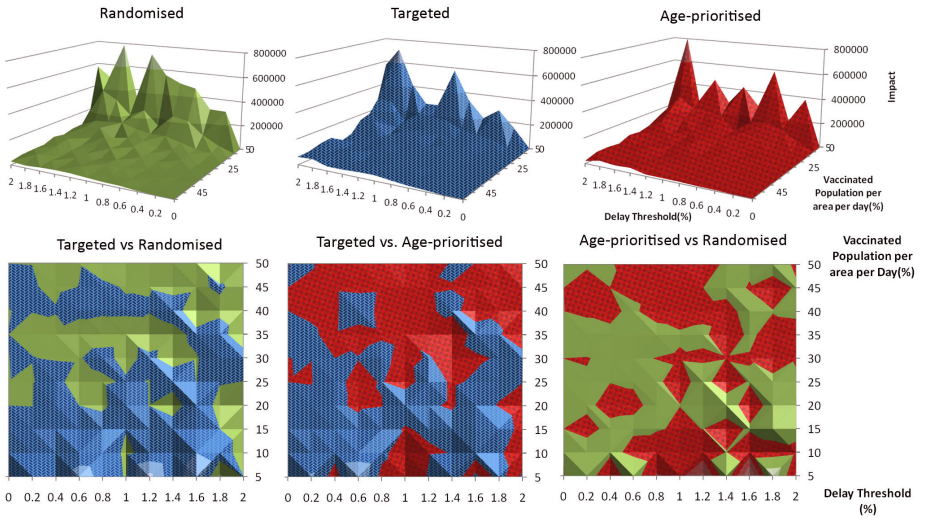

Fig. 4. Performance Comparison between three vaccination strategies

vaccination became less eminent as the delay lengthened. This is understandable in that given the delay, the targeted individuals may have already outnumbered the limited vaccination supply and many of them may have already been exposed. As the constraint on allowed vaccinations loosens, i.e. the vaccination percentage increases, age-prioritised vaccination starts to outperform the other two. This indicates that blindly prioritising the vaccination on one age group may not be beneficial if the daily vaccine provision is limited. Surely this allows ample time for other potential age groups to propagate the disease unless the vaccination is carried out as swiftly as possible.

4 Evaluation and Future Work

In this paper, we described a contact network model for modeling epidemics with emphasis on demographic information. We discussed the parameters of the model and tested three vaccination strategies. We found that targeted vaccination, albeit unrealistic, is a better strategy under normal circumstances but given less constraint on the provision of vaccines, age prioritised vaccination prevails.

An ideal time dependent bipartite graph requires every individual in the system to be in only one place at a reasonably small time step and evolves according to some mobility models. Various analyses of actual human social dynamics exist [17]. When a social mobility model is employed and thereby a more realistic contact network structure is known, the current people-people infection propensity can be refined. To save the computational cost, the time step is one day and once

the people-location bipartite graphs are built they remain unchanged throughout the simulation. This static projection graph is more highly connected than the time dependent version and is thus a safe simplification to make.

Certain virus is known to be able to survive in normal environment for hours and even days. This can be incorporated into our model by imagining a contaminated location as an infective itself, but we think this unnecessarily increases the degrees of freedom in the model and have therefore omitted this phenomenon. Birth rate and death rate (the MSEIR model [5]) are also not considered.

To conclude, both epidemic spreading and vaccination strategies are highly intricate and stochastic. Our model has shown how one infected individual is sufficient in causing a small scale infection that involved only a few people in a few days to a half a year region-wide epidemic. The ultimate aim of any kind of epidemic modeling is to bolster the development of better efficient countermeasure strategies and this will require further insights into social networks, vaccination and virus-specific pathogenesis.

Acknowledgements. This project is supported by EC IST SOCIALNETS project—Grant agreement number 217141.

References

1. Rvachev, L., Longini, I.: Math. Biosci. 75, 3 (1985)
2. Grenfell, B.T., et al.: Nature 414, 716 (2001)
3. Longini, I., et al.: Am. J. Epidemiol. 123, 383 (1986)
4. Meyers, L.A., et al.: J. Theor. Biol. 240, 400 (2006)
5. Hethcote, H.W.: SIAM review 42, 599 (2000)
6. Nagel, K., et al.: Int. J. Complex Systems 244 (1998)
7. Eubank, S.S., et al.: Nature 429, 180 (2004)
8. Ferguson, N.M., et al.: Nature 437, 209 (2005)
9. Epstein, J.M., et al.: Brookings Institute Center on Social and Economic Dynamics Working Paper 31 (2002)
10. Bian, L.: Environment and Planning B: Planning and Design 31, 381 (2004)
11. Brownstein, S.J., et al.: Am. J. Epi. 162, 686 (2005)
12. Hpa national influenza season summary (2007), `http://www.hpa.gov.uk`
13. Bailey, N.T.J.: The Mathematical Theory of Infectious Diseases. Murray, J.D. 2nd edn. Mathematical Biology. Springer, Berlin (1993)
14. Rabenau, H.F., et al.: Med. Microbiol. Immunol. 194, 1 (2005)
15. Lowen, A.C., et al.: PLoS Pathog. 19, 1470 (2007)
16. Bureau of Transportation Statistics Highlights of the 2001 National Household Travel Survey (2003), `http://www.bts.gov/publications/`
17. Eagle, N., Pentland, A.: Personal and ubiquitous computing 10, 255 (2006)